NQR and X-ray Studies of $[N(CH_3)_4]_3M_2X_9$ and $(CH_3NH_3)_3M_2X_9$ (M = Sb, Bi; X = Cl, Br)*

Hideta Ishihara, Koichi Watanabe, and Ayako Iwata

Department of Chemistry, Faculty of Education, Saga University, Honjo-machi 1, Saga 840, Japan

Koji Yamada, Yoshihiro Kinoshita, and Tsutomu Okuda

Department of Chemistry, Faculty of Science, Hiroshima University, Higashisenda-machi, Naka-ku, Hiroshima 730, Japan

V. G. Krishnan, Shi-qi Dou, and Alarich Weiss

Institut für Physikalische Chemie, Physikalische Chemie III, Technische Hochschule Darmstadt, Petersenstr. 20, D-6100 Darmstadt, Germany

Z. Naturforsch. **47a**, 65–74 (1992); received August 3, 1991

^{35}Cl, ^{81}Br, ^{121}Sb, and ^{209}Bi NQR of the title compounds was observed. According to the results of the temperature dependences of NQR frequencies and the DTA measurements, phase transitions take place in $[N(CH_3)_4]_3Bi_2Br_9$ ($T_{tr} = 183$ K), $[N(CH_3)_4]_3Bi_2Cl_9$ ($T_{tr} = 155$ K), and $(CH_3NH_3)_3Bi_2Cl_9$ ($T_{tr} = 200$ and 249 K). ^2D NMR spectra for partially deuterated $(CH_3ND_3)_3Bi_2Br_9$ showed that the phase transitions in this compound are related to the motion of the methylammonium cations. Single-crystal X-ray work at room temperature shows that the space group for $[N(CH_3)_4]_3Sb_2Cl_9$ is $P6_3/mmc$ with $a = 925.1$ pm, $c = 2173.4$ pm, $Z = 2$. For $(CH_3NH_3)_3Sb_2Br_9$ the space group is $P\bar{3}m1$ with $a = 818.8$ pm, $c = 992.7$ pm, $Z = 1$; in both cases the cations show dynamical disorder. The Rietveld analysis of the powder X-ray diffraction for $(CH_3NH_3)_3Bi_2Br_9$ reveals the space group $P\bar{3}m1$ with $a = 821.0$, $c = 1000.4$ pm, $Z = 1$ at room temperature; the compound is isomorphous with $(CH_3NH_3)_3Sb_2Br_9$. The crystal symmetries of the low-temperature phases of $(CH_3NH_3)_3Bi_2Br_9$ and $[N(CH_3)_4]_3Bi_2Br_9$ were deduced from the results of the NQR spectroscopy.

Introduction

In recent years Jakubas et al. [1] have reported that a series of compounds with the general formula $A_3M_2X_9$ (A = alkylammonium cations; M = Sb; X = Cl, Br) exhibit dielectric anomalies and motions of the alkylammonium cations induce the order-disorder type phase transition. At present three types of crystal structures of the compounds with anions $M_2X_9^{3\ominus}$ are known. The first one consists of one-dimensional double chains of polyanions like $(CH_3NH_3)_3Sb_2Cl_9$ [2], the second one shows two-dimensional layers of polyanions, e.g. in $Cs_3Bi_2Br_9$, [3], and the third one is built up of isolated $M_2X_9^{3\ominus}$ anions as found in $[N(CH_3)_4]_3Sb_2Br_9$ [4]. We tried to investigate the structures of $A_3M_2X_9$ in more detailed X-ray diffraction experiments and by observing NQR spectra. We also expect to get more information on the crystal structure in the low-temperature phase from the results of NQR work.

* Presented at the XIth International Symposium on Nuclear Quadrupole Resonance Spectroscopy, London, United Kingdom, July 15–19, 1991.

Reprint requests to Dr. H. Ishihara, Dept. of Chemistry, Faculty of Education, Saga University, Honjo-machi 1, Saga 840, Japan.

Experimental

The title compounds were prepared by adding a solution of alkylammonium halide in concentrated hydrobromic acid or hydrochloric acid to a solution of Sb_2O_3 or Bi_2O_3 in the same solvent in molar ratio of 3:1. The products formed immediately and were recrystallized from hot mother liquor. The antimony or bismuth content (in weight %, found/calculated) is as follows: $(CH_3NH_3)_3Sb_2Br_9$: Sb, 21.7/22.99; $(CH_3NH_3)_3Sb_2Cl_9$: Sb, 36.7/36.96; $[N(CH_3)_4]_3Sb_2Br_9$: Sb, 19.8/20.55; $[N(CH_3)_4]_3Sb_2Cl_9$: Sb, 29.9/31.02; $(CH_3NH_3)_3Bi_2Br_9$: Bi, 33.8/33.88; $(CH_3NH_3)_3Bi_2Cl_9$: Bi, 49.8/50.16; $[N(CH_3)_4]_3Bi_2Br_9$: Bi, 31.5/30.74; $[N(CH_3)_4]_3Bi_2Cl_9$: Bi, 43.0/43.56.

NQR was observed using a superregenerative-type spectrometer and a pulsed NQR spectrometer (MATEC) in the frequency range $8.6 \leqq \nu/\text{MHz} \leqq 130$.

0932-0784 / 92 / 0100-0065 $ 01.30/0. – Please order a reprint rather than making your own copy.

Table 1. NQR frequencies for ν_i for $(CH_3NH_3)_3M_2X_9$ and $[N(CH_3)_4]_3M_2X_9$. M = Sb, Bi; X = Cl, Br. (b): bridging atoms; (t): terminal atoms; (s): strong line intensity. The mean error in the frequency measurement is ±0.03 MHz for Br and ±0.01 MHz for ^{35}Cl, ^{121}Sb, and ^{209}Bi.

Compound	Nucleus	ν_i/MHz		Transition $m \leftrightarrow m+1$
		$T = 77$ K	$T = 298$ K	
$(CH_3NH_3)_3 \cdot Sb_2Cl_9$	^{121}Sb		22.35	
			23.87	
	^{35}Cl		13.25 (t)	
			14.35 (t)	
			14.63 (t)	
			15.06 (t)	
$(CH_3NH_3)_3 \cdot Bi_2Cl_9$	^{209}Bi		9.32	
			9.60	
			14.08	
			18.77	
	^{35}Cl		12.65 (t)	
			12.70 (t)	
			13.04 (t)[d]	
			13.44 (t)	
$[N(CH_3)_4]_3 \cdot Bi_2Cl_9$	^{209}Bi		9.18	
	^{35}Cl		12.84 (t)	
$(CH_3NH_3)_3 \cdot Sb_2Br_9$	^{121}Sb[a]		13.78	±1/2↔±3/2
			27.56	±3/2↔±5/2
	^{81}Br		64.91 (b)	
			101.65 (t)	
$(CH_3NH_3)_3 \cdot Bi_2Br_9$	^{209}Bi[b]		8.86	±5/2↔±7/2
			11.78	±7/2↔±9/2
	^{81}Br	61.10 (b)	65.21 (b)[c]	
		64.35 (b)		
		65.48 (b)		
		67.05 (b)		
		70.34 (b)		
		84.95 (t)	92.57 (t)[c]	
		89.83 (t)		
		92.78 (t)		
		93.36 (t)		
		95.56 (t)		
		96.08 (t)		
		97.28 (t)		
		98.21 (t)		
$[N(CH_3)_4]_3 \cdot Sb_2Br_9$	^{81}Br		39.70 (b)	
			101.67 (t)	
$[N(CH_3)_4]_3 \cdot Bi_2Br_9$	^{209}Bi	13.58	11.98	
		14.94		
	^{81}Br		41.37 (b)	
		91.37 (t)	91.96 (t)	
		94.13 (t, s)		
		97.10 (t, s)		
		97.48 (t)		

[a] $e^2Qqh^{-1}(^{121}Sb) = 91.87$ MHz and $\eta(^{121}Sb) = 0$.
[b] $e^2Qqh^{-1}(^{209}Bi) = 70.71$ MHz and $\eta(^{209}Bi) = 0$.
[c] 65.27 and 92.62 MHz for bridging and terminal bromine atoms in $(CH_3ND_3)_3Bi_2Br_9$.
[d] ^{209}Bi transition not excluded.

The NQR frequencies of the title compounds are listed in Table 1. The assignments of the ^{35}Cl resonances are tentative, because not all quadrupole transitions of the antimony isotopes or ^{209}Bi were observed. ^1H NMR and ^2D NMR spectra were recorded at 22.00 MHz and 9.636 MHz, respectively, using the solid-echo technique. The measurements of differential thermal analysis (DTA) was made using a homemade apparatus.

Table 2. Experimental conditions for the crystal structure determinations and crystallographic data of $[N(CH_3)_4]_3Sb_2Cl_9$ and $(CH_3NH_3)_3Sb_2Br_9$. Diffractometer: Stoe-Stadi 4; Monochromator: Graphite (002); Wavelength: 71.069 pm (MoKα); Scan $\omega/2\Theta$.

Formula, (M)	$[N(CH_3)_4]_3Sb_2Cl_9$ $C_{12}H_{36}Cl_9N_3Sb_2$ (785.01)	$(CH_3NH_3)_3Sb_2Br_9$ $C_3H_{18}Br_9N_3Sb_2$ (1058.83)
Habitus, size	prism, (0.38 × 0.42 × 0.5 mm)^3	prism, (0.50 × 0.50 × 0.60) mm^3
Color	colorless	bright yellow
Temperature/K	299	300
Linear absorption coefficient, μ/m^{-1}	2450	17810
$(\sin\Theta/\lambda)_{max}/pm^{-1}$	0.0054	0.0065
Number of reflections measured	2817	2712
Symmetry independent reflections	445	538
Reflections considered	443	529
Number of parameters	39	16
R (F)	0.078	0.090
R_w (F)	0.072	0.081
Lattice constants		
a/pm	925.1 (3)	818.8 (2)
c/pm	2173.4 (8)	992.7 (3)
Space group	$D^4_{6h} - P6_3/mmc$	$D^3_{3d} - P\bar{3}m1$
Formula units/cell, Z	2	1
$\varrho_{calc}/(Mg \cdot m^{-3})$	1.618 (2)	3.049 (2)
$\varrho_{pyk}/(Mg \cdot m^{-3})$	1.60	2.95
$V_c/(10^6\ pm^3)$	1610.8 (16)	576.4 (5)

The structure of $[N(CH_3)_4]_3Sb_2Cl_9$ and $(CH_3NH_3)_3Sb_2Br_9$ was determined by single crystal X-ray work at room temperature, and experimental details and some crystallographic data are given in Table 2. The structure of $(CH_3NH_3)_3Bi_2Br_9$ was determined by Rietveld analysis of X-ray powder diffraction data; experimental details and crystallographic data are listed in Table 3.

Results and Discussion

Tris-monomethylammonium enneachlorodiantimonate(III), $(CH_3NH_3)_3Sb_2Cl_9$

Six NQR lines were observed at room temperature; two around 23 MHz and four around 14 MHz. They

Table 3. Experimental conditions and crystallographic data of $(CH_3NH_3)_3Bi_2Br_9$. Diffractometer: Rigaku Rad-B; Radiation: CuKα[a]. The Rietveld analysis was made using a dummy atom (potassium) in place of the cation $CH_3NH_3^{\oplus}$, see text.

Formula, (M)	$C_3H_{18}Bi_2Br_9N_3$ (1233.33)
Temperature/K	300
Range 2Θ/°	5.04–85.0
Sweepstep/°	0.04
$R(F)$[b]	0.074
Number of parameters	11
Number of atoms	5
Lattice constants a/pm	821.0 (1)
c/pm	1000.4 (1)
Space group	$D_{3d}^3-P\bar{3}m1$
Number of formula units/cell, Z	1
ϱ_{calc}/(Mg · m^{-3})	3.506 (1)
ϱ_{pyk}/(Mg · m^{-3})	3.30
V_e/(10^6 pm^3)	584.0 (1)

[a] The measurements were made using CuKα radiation (Kα_1 and Kα_2). The Rietveld analysis was done in consideration of the intensity ratio of Kα_1 and Kα_2.

[b] $R(F)=\{\Sigma|[I_k(\text{obs})]^{1/2}-[I_k(\text{calc})]^{1/2}|\}/\Sigma[I_k(\text{obs})]^{1/2}$, where I_k(obs) and I_k(calc) are the integrated intensities.

are listed in Table 1. According to the crystal structure [2], there are four terminal and two bridging chlorine atoms in the asymmetric unit. Considering the Sb–Cl bond length [5] and the bridge angles, the bridging chlorine atoms probably give the resonance lines below 8.5 MHz. Tentatively the two lines around 23 MHz were assigned to the antimony atoms and the four lines around 14 MHz to the four terminal chlorine atoms. The temperature dependence of the ^{121}Sb NQR frequencies and of the two stronger ^{35}Cl lines is shown in Figure 1. With decreasing temperature, one ^{35}Cl line splits into a doublet, and there were deflections in the $\nu(^{35}\text{Cl})=f(T)$ curve for another ^{35}Cl and for one ^{121}Sb NQR line. No heat anomaly was detected in the DTA curve around this temperature. This might be a phase transition, but there is also the possibility that resonance lines coincided accidentally above this temperature. With further decreasing temperature, all resonance lines disappeared below 215 K; there was an endothermic peak in the DTA curve at the same temperature in the heating run. This corresponds to the first-order phase transition reported at 208 K by Jakubas et al. [2].

Tris-monomethylammonium enneachlorodibismuthate (III), $(CH_3NH_3)_3Bi_2Cl_9$

Landers and Brill reported NQR frequencies of this compound but our assignment is different from theirs

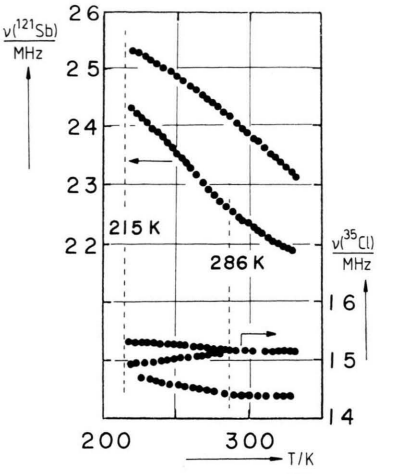

Fig. 1. $(CH_3NH_3)_3Sb_2Cl_9$: ν (^{121}Sb) and ν (^{35}Cl) as functions of temperature.

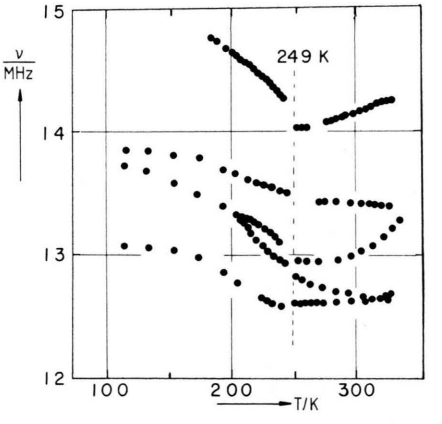

Fig. 2. The temperature dependence of ^{209}Bi and ^{35}Cl NQR frequencies of $(CH_3NH_3)_3Bi_2Cl_9$.

[6]. The compound is isomorphous with the Sb analogue [7] and therefore two nonequivalent Bi atoms, four terminal Cl atoms, and two bridging Cl atoms are expected. Probably the bridging ^{35}Cl atoms give the resonance lines below 8.5 MHz for the same reason given for the bridging atoms in the Sb analogue. The ^{37}Cl NQR lines corresponding to ^{35}Cl NQR lines of 12.65 and 12.70 MHz were observed. We could not assign each ^{209}Bi resonance line to the appropriate quadrupole transition of ^{209}Bi atoms because the complete spectra were not observed. The temperature dependence of the NQR frequencies of ^{35}Cl and ^{209}Bi around 13 MHz is shown in Figure 2. With decreasing temperature, a discontinuity appeared at 249 K. With further decrease two ^{35}Cl resonance lines coincided at

200 K. Below this temperature the number of ^{35}Cl resonance lines decreased from four to three and the intensities of them descended; three ^{35}Cl NQR lines could be observed down to about 110 K. The ^{209}Bi NQR line could be observed down to about 185 K. Small endothermic peaks appeared in the DTA at 249 K and 200 K, respectively. This shows that two phase transitions take place and that the phase transition at 249 K is of first-order, although these two transitions were not observed by infrared spectroscopy and by measurements of the dielectric permitivity [8]. Above 249 K the temperature dependence of NQR frequencies is anomalous. This might be due to the phase transition at 385 K, reported by Jakubas et al. [7].

Tris-tetramethylammonium enneachlorodiantimonate (III), $[N(CH_3)_4]_3Sb_2Cl_9$

No NQR was observed between 77 K and room temperature using the continuous wave method. The experiments have been done at several temperatures. It may be that the NQR lines are very broad, caused by phase transitions. It is reported that two phase transitions take place, at 156 K and at 223 K [9].

The structure of the title compound was determined by single crystal X-ray work. The systematic extinctions show the possible space groups $P6_3mc$, P62c, and $P6_3/mmc$. We chose $P6_3/mmc$, in analogy to the corresponding bromine compound [4]. Using SHELX 86, the crystal structure was solved in approximation. Therefrom the positional parameters of the Sb and Cl atoms followed. The refinement of the atomic position was done with SHELX-76. Difference Fourier maps showed the approximate positions for N and C atoms. We must allocate the carbon atoms to the disorder sites; C(1) and C(2) exhibit three-fold site disorder at 12k and 12j, respectively, and C(4), in general position 24l, is two-fold site disordered as in the case of the Br analogue [4], probably because isotropic rotation of $[N(CH_3)_4]^{\oplus}$ takes place at room temperature like in $[N(CH_3)_4]_3Bi_2Br_9$ as shown later. The atomic positions and thermal parameters are given in Table 4a and some bond distances and angles are listed in Table 4b. The crystal is built up by the tetramethylammonium cations and the discrete anions $Sb_2Cl_9^{3\ominus}$ which is shown in Figure 3.

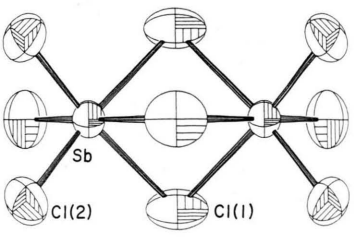

Fig. 3. Structure of the anion $[Sb_2Cl_9]^{3\ominus}$ in tris-tetramethylammonium enneachlorodiantimonate(III). The thermal ellipsoids are shown.

Tris-tetramethylammonium enneachlorodibismuthate (III), $[N(CH_3)_4]_3Bi_2Cl_9$

Two NQR lines were observed at room temperature and a ^{35}Cl NQR line of 12.84 MHz is in agreement with a reported one [6]. The assignment of resonance lines is tentative because the complete spectra were not observed. The temperature dependence of the NQR frequencies is shown in Figure 4. Resonance lines disappeared below 148 K. There was an endothermic peak on the DTA curve at 155 K in the heating run. This shows that the first-order phase transition is accompanied by thermal hysteresis.

Tris-monomethylammonium enneabromodiantimonate (III), $(CH_3NH_3)_3Sb_2Br_9$

It is reported that two phase transitions take place at 131 and 168 K, respectively [10]. The temperature dependence of ^{81}Br NQR frequencies above 168 K was studied by Mackowiak et al. [11]. We observed the temperature dependence of ^{121}Sb NQR frequencies as shown in Figure 5. All resonance lines disappeared below 168 K, and there were two endothermic peaks at 151 K and at 178 K on the DTA curves, in the

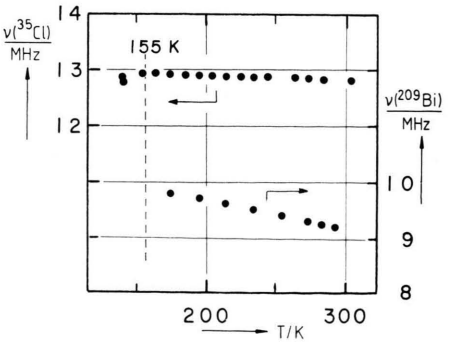

Fig. 4. Temperature dependence of ^{209}Bi and ^{35}Cl NQR frequencies of $[N(CH_3)_4]_3Bi_2Cl_9$.

Table 4a. Positional and thermal parameters (with standard deviation) of $[N(CH_3)_4]_3Sb_2Cl_9$. The U_{ij} are given in $(pm)^2$. U is the isotropic thermal parameter. For F_0, F_c see [21].

Atom	Position[a]	x/a	y/b	z/c	U_{11}, U	U_{22}	U_{33}	U_{12}	U_{13}	U_{23}
Sb	4f	0.3333	0.6667	0.1625 (1)	673 (13)	673 (13)	524 (17)	337 (7)	0	0
Cl (1)	6h	0.4728 (6)	0.9455 (11)	0.2500	1268 (72)	539 (55)	1944 (118)	270 (28)	0	0
Cl (2)	12k	0.2074 (4)	0.4148 (9)	0.0992 (3)	1477 (52)	964 (51)	904 (49)	482 (25)	−128 (21)	−255 (42)
N (1)	2b	0.0000	0.0000	0.2500	739 (124)					
N (2)	4f	0.6667	0.3333	0.0925 (16)	852 (95)					
C (1)	12k	0.1372 (80)	0.0686 (40)	0.2005 (29)	938 (229)					
C (2)	12j	−0.1371 (56)	0.0497 (76)	0.2500	863 (229)					
C (3)	4f	0.6667	0.3333	0.1623 (32)	1900 (288)					
C (4)	24l	0.6961 (41)	0.1910 (43)	0.0738 (15)	1268 (148)					

[a] Wyckoff notation:
24l: x, y, z; $\bar{y}, x-y, z$; $y-x, \bar{x}, z$; $\bar{y}, \bar{x}, z$; $x, x-y, z$; $y-x, y, z$;
$\bar{x}, \bar{y}, \bar{z}$; $y, y-x, \bar{z}$; $x-y, x, \bar{z}$; $y, x, \bar{z}$; $\bar{x}, y-x, \bar{z}$; $x-y, \bar{y}, \bar{z}$;
$\bar{x}, \bar{y}, 1/2+z$; $y, y-x, 1/2+z$; $x-y, x, 1/2+z$;
$x, y, 1/2-z$; $\bar{y}, x-y, 1/2-z$; $y-x, \bar{x}, 1/2-z$;
$y, x, 1/2+z$; $\bar{x}, y-x, 1/2+z$; $x-y, \bar{y}, 1/2+z$;
$\bar{y}, \bar{x}, 1/2-z$; $x, x-y, 1/2-z$; $y-x, y, 1/2-z$.
12k: $x, 2x, z$; $2\bar{x}, \bar{x}, z$; $x, \bar{x}, z$; $\bar{x}, 2\bar{x}, \bar{z}$; $2x, x, \bar{z}$; $\bar{x}, x, \bar{z}$;
$\bar{x}, 2\bar{x}, 1/2+z$; $2x, x, 1/2+z$; $\bar{x}, x, 1/2+z$;
$x, 2x, 1/2-z$; $2\bar{x}, \bar{x}, 1/2-z$; $x, \bar{x}, 1/2-z$.
12j: $x, y, 1/4$; $\bar{y}, x-y, 1/4$; $y-x, \bar{x}, 1/4$; $\bar{y}, \bar{x}, 1/4$;
$x, x-y, 1/4$; $y-x, y, 1/4$;
$\bar{x}, \bar{y}, 3/4$; $y, y-x, 3/4$; $x-y, x, 3/4$; $y, x, 3/4$;
$\bar{x}, y-x, 3/4$; $x-y, \bar{y}, 3/4$.
6h: $x, 2x, 1/4$; $2\bar{x}, \bar{x}, 1/4$; $x, \bar{x}, 1/4$; $\bar{x}, 2\bar{x}, 3/4$; $2x, x, 3/4$; $\bar{x}, x, 3/4$.
4f: $1/3, 2/3, z$; $2/3, 1/3, \bar{z}$; $2/3, 1/3, 1/2+z$; $1/3, 2/3, 1/2-z$.
2b: $0, 0, 1/4$; $0, 0, 3/4$.

Table 4b. Bond distances (pm) and angles (°) with standard deviations in parentheses for $[N(CH_3)_4]_3Sb_2Cl_9$.

	d/pm
Sb−Cl (1)[a]	293.4 (9)
Sb−Cl (2)[b]	244.2 (11)
Sb ··· Sb (^{i})	380.2 (5)
	angle/°
Sb−Cl (1)−Sb (^{i})[c]	80.8 (2)
Cl (2)−Sb−Cl (2^{ii})	91.4 (1)
Cl (1)−Sb−Cl (2^{ii})	92.9 (3)
Cl (1)−Sb−Cl (1^{iii})	82.5 (2)
Cl (1)−Sb−Cl (2)	173.9 (3)

[a] The bridging chlorine atom.
[b] The terminal chlorine atom.
[c] Atoms carrying i, ii, and iii are related to original atoms by the relationships $1/3, 2/3, z \rightarrow 1/3, 2/3, 1/2, -z$; $x, 2x, z \rightarrow x, \bar{x}, z$; and $x, 2x, 1/4 \rightarrow x, \bar{x}, 1/4$; respectively.

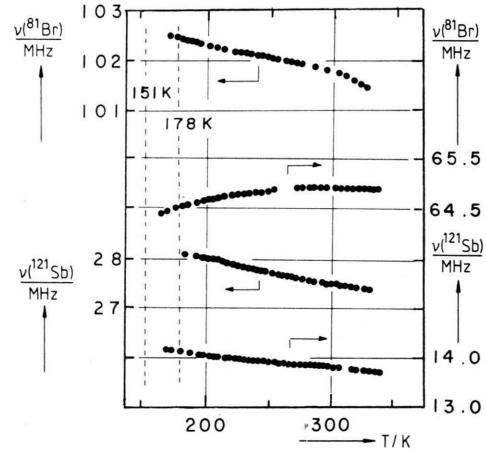

Fig. 5. $(CH_3NH_3)_3Sb_2Br_9$: Temperature dependence of ^{121}Sb and ^{81}Br NQR frequencies.

heating run. The phase transitions seem to be accompanied by thermal hysteresis. Below 168 K each NQR line should be split into several lines, and the low line intensity is probably one reason why no resonance was observed in the low-temperature phase. The crystal structure at room temperature was determined by single-crystal X-ray work. No systematic extinctions were observed. The possible space groups were P3m1, P321, and P$\bar{3}$m1. We selected P$\bar{3}$m1, as already proposed by Jakubas et al. [10]. These authors selected P$\bar{3}$m1 because of the lack of the pyroelectric effect at room temperature. The difference Fourier maps gave only an approximate position of the cation $CH_3NH_3^{\oplus}$ at 1a: (0,0,0). A refinement of the positions for the C, N, and H atoms was not done, because isotropic rotation of cations take place at room temperature [11], as in the Bi analogue, see below. The positions and thermal parameters of the title compound are listed in Table 5a, and some bond distances and angles are given in Table 5b. The compound is isostructural with $Cs_3Bi_2Br_9$ [3] consisting of a two-dimensional layer – polyanion with two cation sites at 1a and 2d.

Table 5a. Positional and thermal parameters (with standard deviation) of $(CH_3NH_3)_3Sb_2Br_9$. The U_{ij} are given in $(pm)^2$. For F_o, F_c see [21].

Atom	Position[a]	x/a	y/b	z/c	U_{11}	U_{22}	U_{33}	U_{12}	U_{13}	U_{23}
Sb	2d	0.6667	0.3333	−0.1861 (3)	380 (11)	380 (11)	304 (14)	190 (6)	0	0
Br (1)	3e	0.5000	0.5000	0.0000	981 (33)	533 (28)	819 (33)	267 (14)	138 (12)	275 (25)
Br (2)	6i	0.3573 (5)	0.1787 (2)	−0.3319 (3)	650 (18)	650 (18)	697 (23)	21 (30)	−302 (17)	302 (17)

[a] Wyckoff notation: 6i: $x, \bar{x}, z$; $x, 2x, z$; $2\bar{x}, \bar{x}, z$; $\bar{x}, x, \bar{z}$; $\bar{x}, 2\bar{x}, \bar{z}$; $2x, x, \bar{z}$. 3e: 1/2, 0, 0; 0, 1/2, 0; 1/2, 1/2, 0. 2d: 1/3, 2/3, z; 2/3, 1/3, $\bar{z}$.

Table 5b. Bond distances (pm) and angles (°) with standard deviations in parentheses for $(CH_3NH_3)_3Sb_2Br_9$.

	d/pm
Sb − Br (1)[a]	300.0 (3)
Sb − Br (2)[b]	262.8 (5)
	angle/°
Sb − Br (1) − Sb (^{i})[c]	180.00
Br (2) − Sb − Br (2^{ii})	92.6 (2)
Br (1) − Sb − Br (2)	90.6 (1)
Br (1) − Sb − Br (1^{iii})	86.1 (1)
Br (1) − Sb − Br (2^{ii})	175.1 (2)

[a] The bridging bromine atom.
[b] The terminal bromine atom.
[c] Atoms carrying i, ii, and iii are related to original atoms by the relationships 2/3, 1/3, $\bar{z} \rightarrow 1/3, 2/3, z$; $2x, x, \bar{z} \rightarrow \bar{x}, x, \bar{z}$; 1/2, 1/2, 0 → 1/2, 0, 0, respectively.

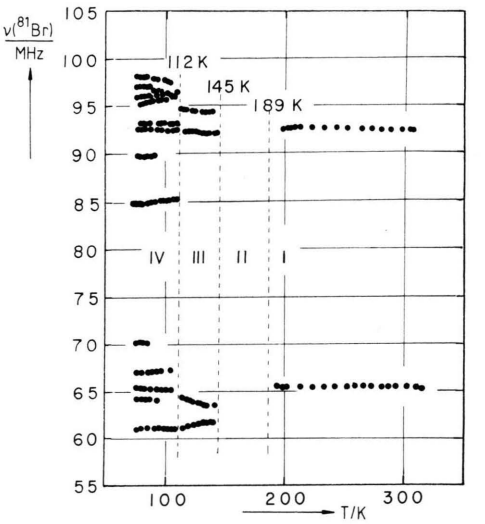

Fig. 6. The temperature dependence of ^{81}Br NQR frequencies in $(CH_3NH_3)_3Bi_2Br_9$.

Tris-monomethylammonium enneabromodibismuthate (III), $(CH_3NH_3)_3Bi_2Br_9$

At room temperature two ^{81}Br NQR lines were observed in agreement with the results of Landers and Brill [6]. $\nu(^{81}Br) = f(T)$ is shown in Figure 6. In the heating run the DTA showed endothermic peaks at 112 K, 145 K, and 189 K (marked by broken lines in Figure 6). Around these transition temperatures the number of ^{81}Br NQR lines decreases stepwise with increasing temperature. The three transitions have been already reported by Jakubas et al. [12]. The phases are named I, II, III, and IV in the order beginning with the room temperature phase. Because of the large line width, ^{81}Br NQR spectra below 189 K were observed by detecting the spin echo signals. In phase II, no Br NQR line was seen, probably because the electric field gradients (EFGs) at the bromine sites are either disturbed due to the onset of cationic motion or modulated by cationic motions.

The temperature dependence of the second moment M_2 of ^1H NMR spectra is shown in Figure 7. In phase IV the rotation of the cations about the C−N axis takes place; the calculated second moment M_2 for the rotation of $CH_3NH_3^{\oplus}$ about the C−N axis [2] is $6.3 \times 10^{-8}\ T^2$, considering intramolecular contribution only. In phase I the cations rotate isotropically. We also observed the temperature dependence of the quadrupolar splitting of ^2D NMR spectra in a partially deuterated sample (cations $CH_3ND_3^{\oplus}$) and the results are shown in Figure 8. One recognizes the important role the cations play in the phase transitions. In phase IV the ^2D-quadrupolar splitting is about 40 kHz, that is the $CH_3ND_3^{\oplus}$ ions rotate about the C−N bond [11]. With increasing temperature the spectrum became more complex. In phase II it consists of two components with splittings of about 30 kHz and 5 kHz, respectively, and the outer splitting became smaller with increasing temperature. In phase I there are two components recognized with splittings of 10 kHz and 5 kHz, respectively, and this is in accordance with the fact that there are two cation sites of phase I. Although we have not analyzed in detail

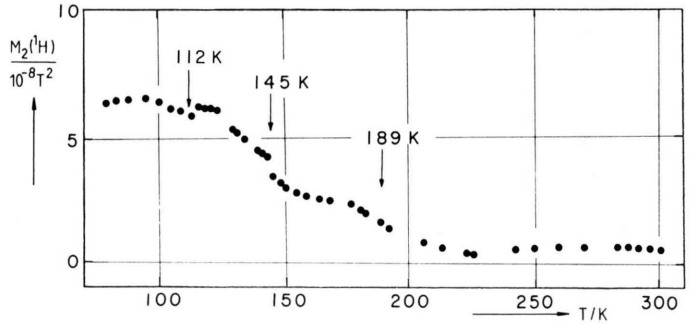

Fig. 7. Temperature dependence of the second moment M_2 of the ^1H NMR in $(CH_3NH_3)_3Bi_2Br_9$.

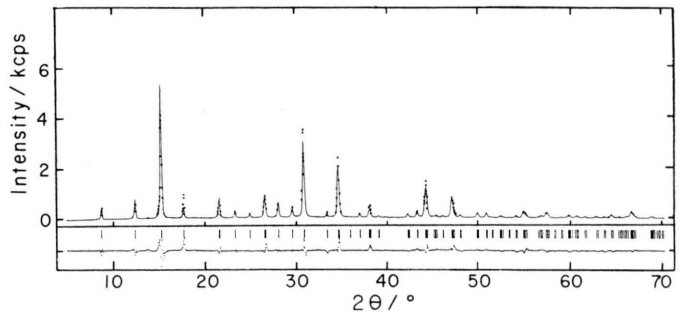

Fig. 9. Final difference plot of the Rietveld analysis of $(CH_3NH_3)_3Bi_2Br_9$. In the upper portion the observed data are shown by dots; the calculated pattern is given by the solid line. The lower part is a plot of the difference. The intensity is given in kilocounts per second.

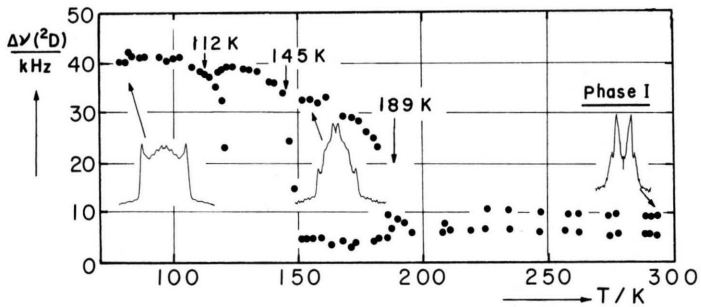

Fig. 8. Temperature dependence of the quadrupole splitting measured between the singularities of ^2D NMR spectra in $(CH_3ND_3)_3Bi_2Br_9$ and some measured spectra. The lateral scale of the spectrum of phase I shown is expanded by a factor of 2.5.

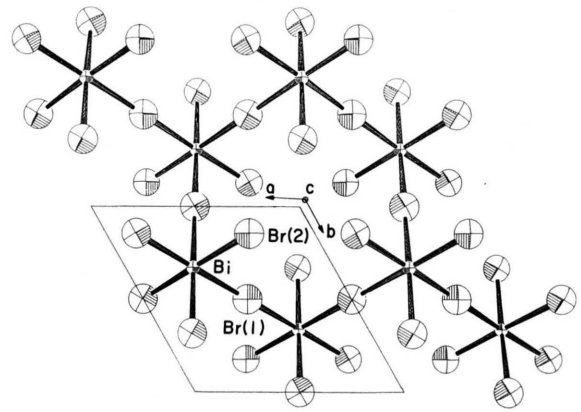

Fig. 10. Projection along the *c*-axis of the anion lattice (layer structure) of $(CH_3NH_3)_3Bi_2Br_9$.

Table 6a. Positional and thermal parameters (with standard deviation) of $(CH_3NH_3)_3Bi_2Br_9$. U is the isotropic thermal parameters given in $(pm)^2$.

Atom	Position	x/a	y/b	z/c	U
Bi	2d	0.6667	0.3333	0.1948 (15)	131 (39)
Br (1)	3e	0.5000	0.5000	0.0000	613 (140)
Br (2)	6i	0.3235 (26)	0.1617	0.3285 (24)	557 (68)
K (1)[a]	1a	0.0000	0.0000	0.0000	2181 (792)
K (2)[a]	2d	0.6667	0.3333	0.6839 (139)	3862 (603)

[a] These K atoms are used as dummy atoms for the refinement.

Table 6b. Bond distances (pm) and angles (°) with standard deviations in parentheses for $(CH_3NH_3)_3Bi_2Br_9$.

	d/pm
Bi – Br (1)[a]	306.9 (15)
Bi – Br (2)[b]	278.3 (33)
	angle/°
Bi – Br (1) – Bi (^{i})[c]	180.0
Br (2) – Bi – Br (2^{ii})	98.8 (9)
Br (1) – Bi – Br (2)	88.1 (7)
Br (1) – Bi – Br (1^{iii})	84.0 (4)
Br (1) – Bi – Br (2^{ii})	169.3 (9)

[a] The bridging bromine atom.
[b] The terminal bromine atom.
[c] Atoms carrying i, ii, and iii are related by the relationships 2/3, 1/3, $\bar{z} \rightarrow 1/3$, 2/3, z; $2x$, x, $\bar{z} \rightarrow \bar{x}$, x, $\bar{z}$; and 1/2, 1/2, $0 \rightarrow 1/2$, 0, 0; respectively.

the line shapes including the information therefrom about the motions and the asymmetry of the EFGs, in phase I the asymmetric parameters of EFGs at ^2D sites produced by outer surrounding charges should be zero, because of the each site symmetry and the isotropic rotations of cations.

To get the crystal structure parameters we tried to analyze the X-ray powder diffraction pattern by the Rietveld method [13]. Dummy potassium atoms were used instead of the $CH_3NH_3^{\oplus}$ cations, because the latter ones execute isotropic rotation at room temperature and K atom is isoelectronic to $CH_3NH_3^{\oplus}$. Figure 9 shows the final best fit profiles obtained by the Rietveld method together with the raw data. The atomic coordinates and the isotropic thermal parameters are listed in Table 6a, some bond distances and angles in Table 6b. The projections along the hexagonal c-axis of the layer structure of the anion is shown in Figure 10. The structure is isomorphous with the Sb analogue and with $Cs_3Bi_2Br_9$, and there are two kinds of $CH_3NH_3^{\oplus}$ ions in the crystal. The EFG at each cation site was calculated using Bertaut's method [14] with the structure parameters obtained, and electric charges +1.831e for Bi, −0.797e for bridging Br, −0.712e for terminal Br and +1e for the cations, deduced from the NQR results. The imbalance of bromine 4p-electrons was calculated from the equation

$$|(e^2 Q q_{obs})/(e^2 Q q_p)| = 2 - N_z \quad (1)$$

for the terminal and bridging Br atoms, respectively [15], and the net charge is equal to $1 - N_z$ for each Br atom. The results of the lattice summation, taken over a volume of ± six lattice constants in each direction, leads to the nuclear quadrupole coupling constants (NQCCs) of 3.54 KHz for ^2D at the point position 1a and of 1.46 KHz for ^2D at 2d. No antishielding factor is taken into account. The quadrupolar splittings observed at room temperature can be reproduced by multiplying the experimental values by a factor of about 4, assuming asymmetric parameters are equal to zero. We consider the ^2D NMR spectra at room temperature as a two component spectrum with different magnitudes of quadrupolar splitting and conclude therefrom an isotropic rotation of the cations with a very small electric field gradient at the deuterium sites.

From the number of the ^{81}Br NQR lines in each phase conclusions about the crystal symmetry can be drawn. In phase III two ^{81}Br NQR lines for the terminal bromines and two lines for the bridging atoms were observed, with an intensity ratios of about 2:1 for both, Br_{ter} and Br_{br}. Therefore, the polyanion contains a mirror plane m. These findings can be explained on the basis of a monoclinic unit cell of double size and a space group symmetry such as $C2/m$. The trigonal unit cell has higher symmetry elements than m and for the atomic positions the unit cell has to be doubled, in comparison to the room temperature structure. Although thirteeen NQR lines were observed in phase IV, they did not appear in the continuous wave experiment and they gave only very weak echoes in the pulse experiment. Therefore we could not decide about the exact number of NQR lines. Jakubas et al. [12] reported the phase IV to be an improper ferroelectric; consequently, the crystal, phase IV, has no inversion center. We consider a lowering of the crystal symmetry from $2/m$ to m in phase IV; the space group of the structure may be Pm, from which eight ^{81}Br NQR lines can be expected for terminal bromines and four lines for the bridging Br atoms.

Considering together with the results of the ^1H- and ^2D NMR measurements, in phase III the $CH_3NH_3^{\oplus}$ ions in position 1a execute isotropic tumbling in advance of the cations in 2d; the ^2D NMR spectra show two components, although the exact area ratios were not determined and the effect of T_1's on the spectra must be considered to get them, and then in phase III the compound has gained an inversion center in the unit cell, wherefrom the symmetry $2/m$ follows for the polyanion. In phase II the cations $CH_3NH_3^{\oplus}$ start isotropic rotation, too, and then the three-fold symmetry of the room temperature unit cell appears.

The exchange of ^1H by ^2D within the NH_3 group of the methylammonium cation induces a positive shift of the ^{81}Br NQR frequencies, 60 kHz at 298 K for both lines. There is, however, within the limits of error in the temperature measurements (± 1.5 K), no shift in the transition temperature T_{tr}.

Tris-tetramethylammonium enneabromodiantimonate (III), $[N(CH_3)_4]_3Sb_2Br_9$

At room temperature, two ^{81}Br NQR lines were observed in the title compound, in accordance with crystal structure work [4]. $\nu(^{81}Br) = f(T)$ is shown in Figure 11. Below 186 K no resonance line was observable; in the heating run, DTA showed an endothermic peak at this temperature. Jakubas et al. reported a phase transition in the title compound at 174 K [9].

Tris-tetramethylammonium enneabromodibismuthate (III), $[N(CH_3)_4]_3Bi_2Br_9$

The temperature dependence of the frequencies of ^{209}Bi and ^{81}Br NQR lines is plotted in Figure 12. With decreasing temperature, the ^{81}Br NQR singlet, observed at room temperature and assigned to the terminal bromines, splits into a quartet and the ^{209}Bi NQR singlet changes to a doublet at 183 K. On the other hand, no resonance line for bridging bromines was detected by searching with spin echo technique at $T \leqq 183$ K. An endothermic peak appears on the DTA curve at 183 K. From these observations it follows that a first order phase transition takes place at this temperature. With rising temperature, from 77 K on, the NQR lines disappeared at around 100 K in coincidence with the temperature of sudden decrease of M_2 (^1H) from 27×10^{-8} T^2 at 85 K to 0.9×10^{-8} T^2 at 112 K. It is apparent that below this temperature range the tetramethylammonium ions are practically

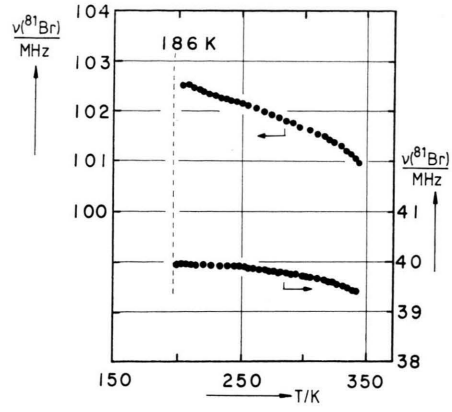

Fig. 11. Temperature dependence of ^{81}Br NQR frequencies in $[N(CH_3)_4]_3Sb_2Br_9$.

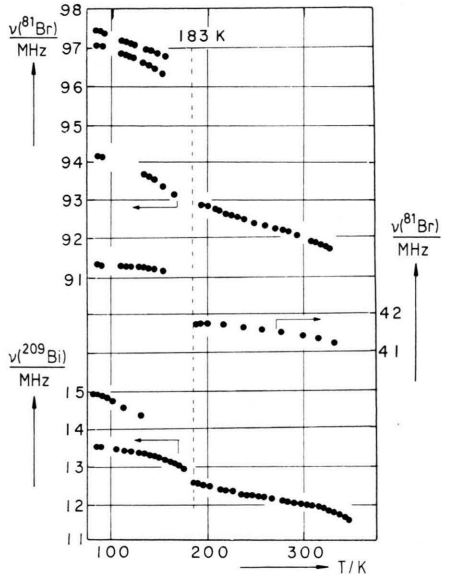

Fig. 12. ^{209}Bi and ^{81}Br NQR frequencies of $[N(CH_3)_4]_3Bi_2Br_9$ as functions of temperature.

rigid in the lattice, including the frozen in CH_3-group rotation; above this temperature isotropic reorientation takes place. Such NMR results are known in literature e.g. for $[N(CH_3)_4]X$ (X = Cl, Br, I [16]; X = $CdCl_3$ [17]). The disappearance of ^{81}Br NQR lines around 100 K is due to the onset of these cation reorientations. Preliminary results of a Rietveld analysis of X-ray powder diffraction data show that the space group of the title compound at room temperature is $P6_3/mmc$, $Z = 2$, $a = 952$ pm, $c = 2246$ pm; the compound is isomorphous to $[N(CH_3)_4]_3Sb_2Br_9$.

The NQR results prove the isomorphism: The same number of ^{81}Br resonance lines was observed in both compounds. In addition, the bridging bromine frequencies in $[N(CH_3)_4]_3M_2Br_9$ (M = Sb and Bi), about 40 MHz at 300 K, are lowered with respect to those frequencies, around 65 MHz, in corresponding $(CH_3NH_3)_3M_2Br_9$ compounds. This observation implies that the bridging angle M–Br–M in $[N(CH_3)_4]_3M_2Br_9$ is about 90° in comparison to the angles 180° in $(CH_3NH_3)_3M_2Br_9$. The bridging bromine frequencies of the latter compounds should be two times larger than one expects, considering the bond distance only [18–20].

In the low temperature phase four NQR lines of the terminal bromines (two with higher, two with lower intensity observed) and two resonance lines of ^{209}Bi were observed. This implies that $[Bi_2Br_9]^{3\ominus}$ has symmetry *m* in a monoclinic space group e.g. Cm, $Z = 2$.

Acknowledgement

We are grateful to the Fonds der Chemischen Industrie for support of this work. Hideta Ishihara expresses his thanks to the Alexander von Humboldt-Stiftung and to the Yamada Science Foundation for a research fellowship.

[1] R. Jakubas and L. Sobczyk, Ferroelectrics **78,** 69 (1988).
[2] R. Jakubas, Z. Czapla, Z. Galewski, L. Sobczyk, O. J. Zogal, and T. Lis, Phys. Status Solidi **A 93,** 499 (1986).
[3] F. Lazarini, Acta Cryst. **B 33,** 2961 (1977).
[4] M. Hall, M. Nunn, M. Begley, and D. B. Sowerby, J. Chem. Soc. Dalton Trans. **1986,** 1231.
[5] H. Ishihara, J. Sci. Hiroshima Univ. Ser. **A 45,** 319 (1981).
[6] A. G. Landers and T. B. Brill, Inorg. Chem. **19,** 744 (1980).
[7] R. Jakubas, J. Zalenski, and L. Sobczyk, Ferroelectrics **108,** 109 (1990).
[8] G. Bator, R. Jakubas, and M. Malarski, J. Molec. Struct. **246,** 193 (1991).
[9] R. Jakubas, Z. Galewski, L. Sobczyk, and J. Matuszewski, Ferroelectrics **88,** 83 (1988).
[10] R. Jakubas, Z. Galewski, L. Sobczyk, and J. Matuszewski, J. Phys. C: Solid State Phys. **18,** L857 (1985).
[11] M. Mackowiak, N. Weiden, and Al. Weiss, Phys. Status Solidi **A 119,** 77 (1990).
[12] R. Jakubas, U. Krzewska, G. Bator, and L. Sobczyk, Ferroelectrics **77,** 129 (1988).
[13] H. M. Rietveld, J. Appl. Crystallogr. **2,** 65 (1969). F. Izumi, M. Mitomo, and Y. Bando, J. Mater. Sci. **19,** 3115 (1984). The analysis was made using the "RIETAN" program, written by F. Izumi.
[14] E. F. Bertaut, J. Phys. Chem. Solids **39,** 97 (1978). H. Nakayama, N. Nakamura, and H. Chihara, J. Phys. Soc. Japan **56,** 2927 (1987).
[15] K. Yamada, T. Matsui, T. Tsuritani, T. Okuda, and S. Ichiba, Z. Naturforsch. **45a,** 307 (1990).
[16] M. Mahajan and B. D. Nageswara Rao, J. Phys. Chem. Solids **33,** 2191 (1972).
[17] Tung Tsang and D. B. Utton, J. Chem. Phys. **64,** 3780 (1976).
[18] T. P. Das and E. L. Hahn, Nuclear Quadrupole Resonance Spectroscopy, in Solid State Physics, Suppl. **1** (1958).
[19] T. Okuda, H. Ishihara, K. Yamada, M. Hiura, and H. Negita, J. Molec. Struct. **74,** 347 (1981).
[20] H. Ishihara, Shi-qi Dou and Al. Weiss, Ber. Bunsenges. Phys. Chem. **95,** 659 (1991).
[21] Further information on the crystal structure determination may be obtained from Fachinformationszentrum Karlsruhe, Gesellschaft für wissenschaftlich-technische Information mbH, D-7514 Eggenstein-Leopoldshafen 2, Germany. Inquiries should be accompanied by the depository number CSD-55596, the names of the authors, and full literature reference.